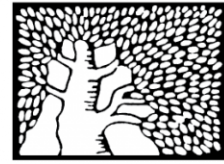


מכון ויצמן למדע

WEIZMANN INSTITUTE OF SCIENCE



## Rho-Associated Coiled-Coil Kinase 1 Translocates to the Nucleus and Inhibits Human Cytomegalovirus Propagation

### Document Version:

Accepted author manuscript (peer-reviewed)

### Citation for published version:

Eliyahu, E, Tirosh, O, Dobesova, M, Nachshon, A, Schwartz, M & Stern-Ginossar, N 2019, 'Rho-Associated Coiled-Coil Kinase 1 Translocates to the Nucleus and Inhibits Human Cytomegalovirus Propagation', *Journal of Virology*, vol. 93, no. 19, 00453-19. <https://doi.org/10.1128/JVI.00453-19>

Total number of authors:

6

### Digital Object Identifier (DOI):

[10.1128/JVI.00453-19](https://doi.org/10.1128/JVI.00453-19)

### Published In:

Journal of Virology

### License:

CC BY-NC

### General rights

@ 2020 This manuscript version is made available under the above license via The Weizmann Institute of Science Open Access Collection is retained by the author(s) and / or other copyright owners and it is a condition of accessing these publications that users recognize and abide by the legal requirements associated with these rights.

### How does open access to this work benefit you?

Let us know @ [library@weizmann.ac.il](mailto:library@weizmann.ac.il)

### Take down policy

The Weizmann Institute of Science has made every reasonable effort to ensure that Weizmann Institute of Science content complies with copyright restrictions. If you believe that the public display of this file breaches copyright please contact [library@weizmann.ac.il](mailto:library@weizmann.ac.il) providing details, and we will remove access to the work immediately and investigate your claim.



1     **ROCK1 translocates to the nucleus and inhibits human cytomegalovirus**  
2     **propagation**

3  
4     Erez Eliyahu<sup>1</sup>, Osnat Tirosh<sup>1</sup>, Martina Dobesova<sup>1</sup>, Michal Schwartz<sup>1</sup> and Noam Stern-Ginossar<sup>1\*</sup>

5  
6     <sup>1</sup> Department of Molecular Genetics, Weizmann Institute of Science, Rehovot 76100, Israel.

7     \* To whom correspondence should be addressed; [noam.stern-ginossar@weizmann.ac.il](mailto:noam.stern-ginossar@weizmann.ac.il)

8  
9  
10    **Abstract**

11    Rho-associated coiled-coil kinase (ROCK) protein is a central kinase that regulates numerous  
12    cellular functions, including cellular polarity, motility, proliferation and apoptosis. Here, we  
13    demonstrate that ROCK has antiviral properties and inhibition of its activity results in  
14    enhanced propagation of human cytomegalovirus (HCMV). We show that during HCMV  
15    infection ROCK1 translocates to the nucleus where it localizes adjacent to the viral replication  
16    compartments and co-localizes with the Virus-Induced Chaperone-Enriched (VICE) domain  
17    marker Hsc70. We further reveal that inhibition of myosin, one of the central targets of  
18    ROCK, also increases HCMV propagation, implying that the anti-viral activity of ROCK is  
19    mediated by nuclear activation of the actomyosin network. Finally, we demonstrate that  
20    inhibition of ROCK results in more capsid accumulation in the cytoplasm compared to the  
21    nucleus, indicating ROCK activity might inhibit the efficient egress of HCMV out of the  
22    nucleus. Altogether our findings illustrate ROCK activity restricts HCMV propagation and  
23    suggest this inhibitory effect is mediated by suppression of capsid egress out of the nucleus.

24

25 **Importance**

26 ROCK is a central kinase in cells that regulates numerous cellular functions, including  
27 cellular polarity, motility, proliferation and apoptosis. Here we reveal a novel anti-viral  
28 activity of ROCK1 during infection with HCMV, a prevalent pathogen infecting most of the  
29 population worldwide. We reveal ROCK activity is exerted by translocation to the nucleus  
30 where it localizes to discrete domains, which are reminiscent of the Virus-Induced  
31 Chaperone-Enriched (VICE) domains described in HSV-1. Our findings suggest that ROCK's  
32 anti-viral activity takes place via nuclear activation of the actomyosin network and leads to  
33 inhibition of capsid egress out of the nucleus.

34

35

## 36 **Introduction**

37 As obligate intracellular parasites, viruses require the host cell machineries and resources  
38 to replicate and propagate. In response, mammalian cells have evolved elaborate defense  
39 mechanisms to detect and inhibit viral replication. The innate and acquired immune  
40 systems are effective at reducing the burden of viral disease but additional cellular  
41 activities provide protection from viruses. These functions are mediated by cellular  
42 proteins that are consecutively expressed and called restriction factors. In some cases,  
43 restriction of viral replication may result from a cell-regulatory function rather than direct  
44 interference with the viral replication cycle (1).

45 We previously integrated translation efficiency measurements with measurements of  
46 protein abundance along HCMV infection to identify 65 cellular proteins that presented  
47 profiles which suggested they are targeted for degradation during HCMV infection (2). Since  
48 targeted degradation may indicate biological importance, we hypothesized that some of these  
49 proteins may act as novel HCMV restriction factors. One of the proteins we identified was  
50 the Rho-associated coiled-coil kinase (ROCK)1 protein. ROCK1 and its homologue  
51 ROCK2 are serine/threonine kinases that were initially identified as activated Rho (Rho-GTP)  
52 interacting proteins (3) and are known today to be the major downstream effectors of the  
53 small GTPase RhoA. ROCKs can also be activated, independently of Rho, by several lipids  
54 and by oligomerization, possibly through amino-terminal transphosphorylation (3).

55 Upon activation, ROCKs function as versatile kinases, regulating a plethora of cellular  
56 processes including cellular polarity, motility, proliferation and apoptosis (3–5). One of the  
57 best characterized roles of ROCKs is regulation of actin-filament assembly and contractility.  
58 This is achieved by phosphorylation of different substrates, including LIM  
59 kinase, myosin light chain (MLC) and MLC phosphatase (5). Phosphorylation of LIM kinase  
60 leads to stabilization of actin filaments and phosphorylation of the myosin light chain (MLC)  
61 and inactivation of MLC phosphatase enhance the activity of the motor protein myosin. As a  
62 consequence, ROCK activity enhances actin-myosin contraction (4, 6).

63 In this study, we examined ROCK's function during HCMV infection. By using  
64 specific inhibitors and genetic knock down we reveal that ROCK activity inhibits HCMV  
65 propagation. We further demonstrate that during HCMV infection ROCK1 is recruited to the

66 nucleus to specific Hsc70 containing-nuclear domains. These domains are reminiscent of  
67 Virus-Induced Chaperone-Enriched (VICE) domains characterized in Herpes Simplex Virus 1  
68 (HSV1) infected cells, and were proposed to act as protein quality control centers that  
69 sequester misfolded or modified proteins (7). Moreover, we show that ROCK anti-viral  
70 activity is probably mediated by hyperactivation of actin-myosin contraction, as the  
71 myosin inhibitor, Blebbistatin, also increased HCMV titers. Finally, we demonstrate that  
72 inhibition of ROCK activity enhances both viral gene expression and capsid budding out of  
73 the nucleus, suggesting that ROCK antiviral activity might be related to the regulation of  
74 actomyosin network in the nucleus.

75

## 76 **Results**

### 77 **ROCK inhibition promotes HCMV propagation**

78 Integration of protein production levels (as measured by ribosome profiling) with protein  
79 abundance measurements along HCMV infection suggested that Rho-associated coiled-coil  
80 kinase 1 (ROCK1), a key regulator of actomyosin network and cell polarity, might be  
81 degraded during HCMV infection ((2) and Figure S1A). We previously demonstrated that the  
82 RNA levels of ROCK1 were increased during HCMV infection whereas ROCK1 protein  
83 levels as measured by immunoblotting were reduced ((2) and Figure S1B), supporting our  
84 initial hypothesis that ROCK1 might be degraded during HCMV infection. Since targeted  
85 degradation may indicate biological importance, we wanted to test whether the activity of  
86 ROCK1 is important for HCMV propagation. To this end, we infected fibroblasts with the  
87 HCMV Merlin strain and at 12 hours before infection or 5 hours post infection (hpi) cells  
88 were treated with a potent ROCK inhibitor, Y27632 (8). Importantly, inhibition of ROCK  
89 resulted in more than a 10-fold increase in viral titers (Figure 1A), suggesting ROCK activity  
90 inhibits HCMV propagation. We previously showed the reduction in ROCK1 protein level  
91 occurred only when cells were infected with HCMV Merlin strain but not when cells were  
92 infected with the HCMV laboratory-adapted strain, AD169, in which a 15 kb comprising the  
93 ULb' region (genes UL133–UL150) is deleted (2). We, therefore, tested the effect of ROCK  
94 inhibition on AD169 propagation. In support of a substantial difference between these two  
95 HCMV strains and in agreement with previous findings (9), inhibition of ROCK activity had  
96 no effect on AD169 titers (Figure 1A). We next used an HCMV Merlin strain that contains a  
97 GFP tagged UL32 (UL32-GFP)(10), which allows for fluorescence-based monitoring of  
98 infection by progeny virions. Fibroblasts were infected with UL32-GFP and ROCK  
99 inhibitor was added at different times post infection. Supernatants were collected at 5 days  
100 post infection (dpi) and used to infect fresh wild type fibroblasts and the percentage of GFP  
101 positive cells was measured by microscopy and flow cytometry, as proxy for viral titers.  
102 Utilizing this approach, we could show that inhibiting ROCK activity even at 48 hpi can  
103 increase viral propagation (Figure 1B and Figure S1C). Furthermore, inhibition of ROCK by a  
104 different, more selective inhibitor, H1152 (11), also resulted in increase in viral titers  
105 excluding the possibility that the effect we observed is related to off targets effects of the drug

106 we used (Figure S1D and S1E). We further established the effect of ROCK inhibition on viral  
107 titers by knocking down (KD) ROCK expression using siRNAs. We confirmed that ROCK  
108 KD led to a significant reduction in ROCK1 protein expression (Figure S1F). In accordance  
109 with our findings using drugs, ROCK KD resulted in a significant increase in viral titers  
110 following infection with Merlin strain but not with AD169 strain (Figure 1C).

111 To define the infection stage affected by ROCK activity, infected cells were treated  
112 with ROCK inhibitor and viral proteins levels were examined at different time points post  
113 infection (Figure 1D). We observed an elevation in viral protein expression (UL44 and pp28)  
114 compared to the untreated sample only at 72 hpi, indicating ROCK activity inhibits late stages  
115 of HCMV propagation. In agreement with a late inhibitory effect, we did not observe major  
116 differences in the levels of viral DNA replication when ROCK activity was inhibited (Figure  
117 1E).

118

### 119 **ROCK1 is translocated to the nucleus during HCMV infection**

120 Given ROCK's anti-viral activity, we sought to determine if ROCK1 is indeed degraded in  
121 HCMV-infected cells. Cells were infected with Merlin strain and were then treated with  
122 inhibitors of the proteasome (MG132) or lysosome (folimycin). Surprisingly, inhibition of  
123 proteasomal or lysosomal degradation did not affect the levels of ROCK1 as assessed by  
124 immunoblotting (Figure 2A and data not shown), indicating that ROCK1 is not actively  
125 degraded by the proteasome or lysosome in HCMV infected cells.

126 We therefore aimed to confirm the reduction in ROCK1 protein levels detected by  
127 western blot analysis, in an alternative method and to inspect its localization during HCMV  
128 infection. We probed for ROCK1 expression using immunofluorescence in mock cells and in  
129 cells infected with Merlin or AD169 strains. Remarkably, infection with Merlin, but not with  
130 AD169, resulted in translocation of ROCK1 into well-defined nuclear domains (Figure  
131 2B). Subcellular fractionation and immunoblotting analysis confirmed that in mock- and  
132 AD169- infected fibroblasts, ROCK1 was predominantly located in the cytoplasmic fractions  
133 whereas in Merlin infected fibroblasts, a significant portion of ROCK1 was detected in the  
134 nuclear fraction (Figure 2C). Notably, the reduction in ROCK1 levels we measured by  
135 immunoblotting occurred at a similar time along infection as its nuclear localization (Figure



136 S2). We further tested if this translocation of ROCK1 into the nucleus occurs in additional  
137 cell types. Epithelial RPE-1 cells were infected with Merlin strain and although as expected  
138 the infection was very inefficient (12, 13), ROCK1 was also observed in well-defined nuclear  
139 domains in cells that were infected (identified by pp28 staining, Figure 2D).

#### 140 **ROCK1 localizes to nuclear insoluble domains**

141 Since our previous immunoblot analysis suggested that ROCK1 protein levels are reduced  
142 during HCMV infection ((2) and Figure S1B), we hypothesized that the nuclear puncta we  
143 observed by microscopy might be partially insoluble and therefore affected our ability to  
144 detect ROCK1 protein in infected cells using immunoblotting. To test this hypothesis, we  
145 harvested mock-infected cells and cells infected with Merlin or AD169 HCMV strains, and  
146 lysed them using mild or harsh lysis conditions. When using mild lysis conditions, the  
147 detection of ROCK1 by immunoblotting was reduced in cells infected with Merlin strain but  
148 not with AD169 strain, compared to mock-infected cells (Figure 3A). This reduction in  
149 ROCK1 detection was not simply due to inefficient extraction of nuclear fractions as we  
150 obtained comparable levels of UL57 (a viral protein that resides in the nuclear replication  
151 compartment). When harsh lysis conditions were used we did not detect any reduction in  
152 ROCK1 expression (Figure 3A), supporting the assumption that the puncta-localized ROCK1  
153 is partially insoluble.

154 To further examine if ROCK1 localizes to insoluble nuclear domains during HCMV  
155 infection we tested if it could be extracted from cells using a detergent buffer wash, as it was  
156 previously demonstrated that nuclear inclusions are resistant to this short detergent extraction  
157 (7, 14). Indeed, we observed that in HCMV-infected cells ROCK1 was resistant to detergent  
158 treatment (compare Figure 3B lower and upper panels), whereas pp28 and UL57 were  
159 efficiently extracted from the cytoplasm and the nucleus (Figure 3B and Figure S3). We  
160 conclude that in Merlin-infected cells ROCK1 localizes to nuclear domains that are partially  
161 insoluble and therefore resemble nuclear inclusions.

#### 162 **ROCK1 co-localizes with VICE domain marker Hsc70**

163 In HCMV-infected cells, viral gene expression, DNA replication and encapsidation occur in  
164 large nuclear structures designated as viral replication compartments. To examine ROCK1  
165 localization relative to the replication compartment we stained HCMV-infected cells for

166 ROCK1 together with metabolic labeling of nascent viral DNA using 5-ethynyl-2'-  
167 deoxyuridine (EdU) that was visualized using Click chemistry or with co-staining for UL57,  
168 which is found throughout the viral replication compartment. These co-staining demonstrated  
169 that ROCK1 localized to defined regions that are adjacent to the viral replication compartment  
170 (Figures 4A and 4B).

171 In Herpes Simplex Virus type 1 (HSV1) infected cells, it was demonstrated that  
172 cellular chaperone proteins such as Hsc70 are translocated to the nucleus and organize into  
173 Virus-Induced Chaperone-Enriched (VICE) domains (7, 15–18). Similar to our observations  
174 about ROCK1, VICE domains in HSV1 infected cells are formed adjacent to nuclear viral  
175 replication compartment and were shown to be resistant to detergent extraction (7). In HCMV  
176 infected cells components of the ubiquitin–proteasome system (UPS) were demonstrated to  
177 assemble into domains at the periphery of replication compartments (19, 20), suggesting  
178 similar structures might be generated during HCMV infection.

179 We therefore examined whether ROCK1 is localized to structures which are similar to  
180 VICE domains. To this end we stained mock- and HCMV-infected cells for Hsc70, a marker  
181 that was used to label VICE domains in HSV1 infected cells (15, 16). In HCMV infected cells  
182 a portion of the Hsc70 protein was translocated to specific puncta in nucleus and this puncta-  
183 localized Hsc70 co-localized with ROCK1 (Figure 4C). These results indicate that ROCK1  
184 localizes to domains similar to VICE domains during HCMV infection.

### 185 **ROCK inhibition enhances virus egress out of the nucleus**

186 We next wanted to elucidate how ROCK inhibition enhances HCMV propagation. It was  
187 previously demonstrated that ROCK inhibition reduces cellular apoptosis (21). Therefore, a  
188 simple explanation for the enhanced viral production when ROCK is inhibited could stem  
189 from improved cell survival. However, using both PI staining and XTT assay, we did not  
190 observe any differences in cell viability when HCMV infected cells were treated with ROCK  
191 inhibitor (Figure 5A and Figure S4). ROCK activity enhances intracellular contractive forces  
192 via the actomyosin network (22). To test if the anti-viral activity of ROCK is related to  
193 actomyosin-mediated contractility we tested the effects of the myosin inhibitor, Blebbistatin,  
194 on HCMV propagation. Notably, similarly to ROCK inhibition, inhibition of myosin activity

195 resulted in enhancement of Merlin but not AD169 propagation (Figure 5B), indicating the  
196 anti-viral activity of ROCK might be related to the activation of the actomyosin network.

197 Since the actomyosin network can affect nuclear organization, we next tested if ROCK  
198 inhibition disrupts the formation of VICE-like domains by analyzing Hsc70 localization.  
199 Inhibition of ROCK did not affect Hsc70 localization to nuclear domains (Figure 5C),  
200 although we verified it abolished the phosphorylation of MLC (Figure S5), illustrating ROCK  
201 activity is probably not important for the generation Hsc70 containing domains. Furthermore,  
202 we could identify nuclear domains containing Hsc70 in cells infected with the HCMV AD169  
203 strain (Figure 5D), in which ROCK1 is not recruited to the nucleus (Figure 2B), supporting  
204 the conclusion that ROCK activity is not involved in the formation of VICE-like Hsc70  
205 containing domains. In contrast, we noticed that inhibition of ROCK activity resulted in less  
206 recruitment of ROCK1 itself into the nucleus (Figure 5E), suggesting that ROCK1  
207 translocation to the nucleus is dependent in its activity.

208 The observation that ROCK inhibition reduced its nuclear localization pointed out that  
209 ROCK anti-viral activity is likely related to its nuclear localization. Furthermore, our results  
210 indicated that ROCK activity inhibits late stages of HCMV replication and is involved in the  
211 activation of the actomyosin network. We therefore sought to determine whether ROCK  
212 inhibition affects the nuclear egress of HCMV which was recently shown to depend on  
213 nuclear actin filaments (23). Subcellular fractionation and immunoblotting analysis  
214 demonstrated that UL32, a tegument protein that associates with HCMV capsids (24), was  
215 more abundant in the cytoplasmic fraction when ROCK was inhibited (Figure 5F). This result  
216 indicates that inhibition of ROCK activity probably leads to more efficient exit of HCMV  
217 capsids out of the nucleus. Over all, our results demonstrate that during infection with HCMV  
218 using a wild type strain, such as Merlin, ROCK1 kinase restricts HCMV propagation. We  
219 propose a mechanism by which ROCK1 translocates to the nucleus where it activates the  
220 actomyosin network and this process inhibits late viral gene expression the efficient exit of  
221 HCMV capsids out of the nucleus.

222 **Discussion**

223 In this study, we first reveal that ROCK activity restricts HCMV propagation as inhibition of  
224 ROCK resulted in a significant 10-fold increase in viral titers. Interestingly we show that  
225 during HCMV infection ROCK1 translocates to the nucleus, where it localizes to nuclear  
226 domains that are insoluble and contain Hsc70, therefore show resemblance to the VICE  
227 domains that were previously characterized in HSV1-infected cells (7). Although ROCK1  
228 localizes to VICE-like domains, our experiments suggest its activity is not required for these  
229 domains' formation, and it is likely that they are functionally independent. Nevertheless, it is  
230 still possible that ROCK activity plays a role in recruiting substrates to this still enigmatic  
231 compartment. Our experiments do reveal, however, that inhibition of ROCK partially blocks  
232 its own recruitment to the nucleus. This result, together with the observations that during  
233 infection with HCMV AD169 strain ROCK1 is not recruited to the nucleus and does not  
234 affect viral titers, suggests that ROCK anti-viral activity is nuclear.

235 ROCK's activity was previously studied in the context of infections revealing plethora  
236 of effects. In the case of Equine Herpesvirus 1 (EHV1) and HSV1 ROCK inhibition inhibited  
237 viral entry (25, 26). For EHV1 the importance of ROCK activity was tested for two different  
238 entry pathways, direct fusion and endocytic pathway. In both, ROCK was critical for  
239 infection, suggesting ROCK is not required for the initial penetration step but to later stages  
240 of entry (26). ROCK activity was also demonstrated to have opposing roles in infection-  
241 induced cell motility. It was demonstrated that vaccinia virus induces cell motility through  
242 inhibiting both ROCK and mDia (27). In contrast, during HCMV infection of vascular  
243 smooth muscle cell, a viral encoded chemokine, US28, was shown to induce cell motility. In  
244 this case inhibition of ROCK activity blocked US28-induced cellular migration, suggesting  
245 ROCK signaling is important for US28-mediated cellular migration (28). Our observations  
246 indicate an anti-viral activity of ROCK, which seems to be unrelated to these previously  
247 described infection related functions of ROCK. In support of our findings that ROCK activity  
248 inhibits HCMV propagation, a recent siRNA screen that examined the effects of membrane  
249 organization factors on HCMV propagation revealed that KD ROCK1 significantly increase  
250 HCMV titers (29).

251 ROCKs act as kinases that phosphorylate various substrates, including MLC and LIM  
252 kinase (3) and one of ROCK's central roles is to regulate actomyosin contractility.  
253 Interestingly, we reveal that treating HCMV infected cells, following viral entry, with the  
254 myosin inhibitor, Blebbistatin, induces viral titers to similar extent as ROCK inhibition. Also  
255 in the case of myosin inhibition, increased viral titers were observed only when cells are  
256 infected with the Merlin strain but not with the AD169 strain. These results suggest that  
257 ROCK anti-viral activity is probably related to its regulation of the actomyosin network.

258 Actomyosin-mediated contractility is a highly conserved mechanism that generates  
259 mechanical stress in animal cells and is involved in many cellular processes such as changes  
260 in shape, intracellular transport and cell mechanosensing (30). Our results suggest that the  
261 anti-viral activity of ROCK is nuclear and occurs at a late time point of infection. Previously  
262 it was shown that tracking UL32 can be used to track viral processes in infected cells,  
263 including nuclear egress (31). ROCK inhibition leads to a significant elevation of cytoplasmic  
264 UL32 at late time points of infection, suggesting that nuclear egress is inhibited by ROCK  
265 activity.

266 The involvement of nuclear actomyosin network in intranuclear movements of  
267 herpesvirus capsids was previously studied and remains controversial (32). HSV1 capsids  
268 motility in the nucleus were shown to be antagonized by temperature reduction or by  
269 inhibitors of ATP, myosin, or actin (33). In line with these observations it has been shown  
270 that HSV1 and pseudorabies virus (PRV) infections result in the formation of nuclear actin  
271 filaments and HSV1 capsids were shown to associate with nuclear myosin V (34). In contrast  
272 more recent analysis reported that HSV1 and PRV infections remodel nuclear architecture so  
273 that capsids can diffuse to the nuclear periphery (35). For HCMV it was demonstrated that  
274 nuclear actin filaments are induced during infection and that these actin filaments are  
275 important for HCMV nuclear egress (23). Furthermore, HCMV capsids were shown to  
276 associate with nuclear myosin V which was required for capsid accumulation in the cytoplasm  
277 and for efficient production of infectious virus (36). Our results add another level of  
278 complexity to these previous findings as we show that inhibition of ROCK and direct  
279 inhibition of Myosin II with Blebbistatin increases viral titers. These results suggest that  
280 nuclear actomyosin activity can also suppress HCMV propagation. However, we cannot  
281 preclude that this is an indirect effect occurring via other cellular processes, such as the

282 mechano-state of the nucleus. It is clear that herpesvirus infection and specifically the  
283 generation of replication compartment poses some major mechanical constraints on the  
284 nucleus. Recent evidence shows that the local mechano-environment within cells can regulate  
285 transcription (37). There is also evidence for roles of nuclear actin and myosin in  
286 transcription, chromatin remodeling, and mRNA export (38, 39). It is therefore possible that  
287 ROCK inhibition relieves a potential stress or constrains on transcription that then affects  
288 viral propagation and viral egress out of the nucleus. Supporting this notion of an indirect  
289 effect is the increase we observed in viral gene expression at 72 hpi when we inhibit ROCK  
290 activity. This increase could not be solely explained by more efficient exit of capsids out of  
291 the nucleus.

292 Another interesting aspect of our findings is the differences we reveal between the  
293 HCMV laboratory-adapted strain, AD169, in which a 15 kb composing the ULb' region  
294 (genes UL133–UL150) is deleted and the Merlin strain that is considered a WT strain with  
295 characterized mutation in only two viral proteins (10). It is well established that there are  
296 drastic differences in the entry pathways different HCMV strains are using (40). Our results  
297 point there might also be ULb'- dependent differences in the way HCMV bud out of infected  
298 cells. Future work will have to delineate the contribution of different viral genes and their  
299 association with ROCK1 entry to the nucleus and anti-viral activity.

300 In summary, we demonstrate that ROCK activity inhibits HCMV propagation at late  
301 stages of infection. Our results indicate that this activity is related to nuclear activation of the  
302 actomyosin network. Our findings and future studies aimed at resolving the role of the  
303 nuclear actomyosin- network for HCMV propagation may be important not just for HCMV  
304 biology but also for general understanding of the potential functions of actomyosin in the  
305 nucleus.

306

307

308

309

310

311 **Acknowledgments:**

312 We thank Stern-Ginossar lab members for critical reading of the manuscript. This research  
313 was supported by the European Research Council starting grant (StG-2014-638142), the  
314 EU-FP7-PEOPLE Career integration grant and the Israeli Science Foundation (1073/14).  
315 NSG is incumbent of the Skirball career development chair in new scientists.

316

317

318

319

320

321

322

323

324

325

326

327

328

329 **Figure legends**

330 **Figure 1. ROCK activity inhibits HCMV propagation**

331 (A) HFF cells were infected with Merlin or AD169 HCMV strains and the ROCK inhibitor  
332 Y27632 or DMSO (as control) were added 12hr before or 5hr post infection. Supernatants  
333 were collected 5 dpi and viral titers were measured by TCID50 assay. (B) HFF cells were  
334 infected with Merlin UL32-GFP strain and were either treated with Y27632 at 5, 24, 48 and  
335 72 hpi, or treated with DMSO. Supernatants were collected at 5 dpi and were used to infect  
336 fresh HFF cells. Viral titers were quantified by measuring percentage of GFP positive cells  
337 using FACS. (C) HFF cells were transfected with an siRNA pool targeting ROCK1 and 2 or a  
338 control siRNA pool and infected with Merlin or AD169 HCMV strains at MOI=3.  
339 Supernatants were collected 5 dpi and were used to infect fresh HFF cells. Viral titers were  
340 quantified by measuring percentage of GFP positive cells using FACS. (D-E) HFF cell were  
341 infected with Merlin strain and ROCK inhibitor (Y26732) was added at 5, 24 and 48 hpi. (D)  
342 Proteins were extracted at the indicated times and analyzed by Western blot analysis with  
343 IE1/2, UL44 and PP28 serving as immediate early, early and late gene markers respectively.  
344 GAPDH was used as a loading control. (E) DNA was extracted 72 hpi and quantified by real-  
345 time PCR using primers for UL55. DNA levels were normalized to the human gene B2M.  
346 Means and error bars (showing standard deviations) represent triplicates. \* p-value<0.05, \*\*  
347 p-value<0.01 by two-sided student's t-test.

348

349 **Figure 2. ROCK1 re-localizes to the nucleus after infection with HCMV Merlin strain**

350 (A) MG132 was added to mock- or Merlin-infected cells at 72 hpi for 5 hours and ROCK1  
351 levels and MHC Class I, which was used as positive control, were analyzed by Western blot.  
352 GAPDH was used as a loading control (B) Fluorescent microscopy images of mock-infected  
353 HFF cells (top) or HFF cells infected with Merlin (middle) or AD169 (bottom) HCMV  
354 strains, and stained with DAPI (blue) and ROCK1 antibody (red) at 72 hpi. (C) Subcellular  
355 localization of ROCK1 protein was examined by cellular fractionation at 72 hpi, separating  
356 between the cytosol and nuclear fractions. Equivalent amount of proteins from the total (T)  
357 cytosol (C) and nucleus (N) fractions were analyzed by western blot for ROCK1, GAPDH  
358 (cytosolic marker) and histone H2B (nuclear marker). Quantification of the ratios of nuclear



359 and cytosolic ROCK1 from two independent experiments is presented. Error bars show  
360 standard deviations. \*\* p-value<0.01 by two-sided student's t-test. **(E)** RPE cells were  
361 infected with HCMV Merlin strain and at 72 hpi stained with DAPI (blue), PP28 (green) and  
362 ROCK1 (red).

363

### 364 **Figure 3. ROCK1 in HCMV infected cells is resistant to detergent treatment**

365 **(A)** Total protein from uninfected HFF cells or HFF cells infected with Merlin or AD169  
366 strains, was extracted 72 hpi using mild or harsh lysis buffers. Protein levels were detected by  
367 Western blot analysis for ROCK1, GAPDH and UL57. **(B)** Fluorescent microscopy images of  
368 Merlin infected HFF cells treated with either PBS or detergent extraction buffer and stained  
369 with pp28 (green) and ROCK1 (red) antibodies and DAPI (blue).

370

### 371 **Figure 4. Nuclear ROCK1 localize to HCMV-induced VICE-like domains**

372 **(A-B)** HFF cells were infected with Merlin strain and stained at 72 hpi for ROCK1 (red) and  
373 DAPI (blue). Replication compartments were imaged by either metabolically labeling nascent  
374 DNA with ethynyl-2'-deoxyuridine (EDU) and attaching a fluorophore by "Click" chemistry  
375 (green) **(A)** or by staining for UL57 (green) **(B)**. **(C)** HFF cells were mock-infected or  
376 infected with Merlin strain and stained at 72 hpi for ROCK1 (red), HSC70 (green) and DAPI  
377 (blue).

378

### 379 **Figure 5. ROCK activity blocks viral egress out of the nucleus**

380 **(A)** Merlin infected HFF cells were harvested at 5 dpi, stained with PI (Propidium iodide) and  
381 analyzed by FACS. Means and standard deviations of triplicates are represent. **(B)** HFF cells  
382 were infected with Merlin UL32-GFP or AD169-GFP HCMV strains and ROCK inhibitor  
383 (Y27632) or myosin inhibitor (blebbistatin) were added 5 hpi. Supernatant were collected at 5  
384 dpi and used to infect fresh HFF cells. Viral titers were quantified by measuring percentage of  
385 GFP positive cells using FACS. Means and standard deviations of triplicates are represent.  
386 **(C)** HFF cells were infected with Merlin HCMV strain and treated with ROCK inhibitor  
387 (Y26732) or DMSO (as control) at 5 hpi and stained 72 hpi with DAPI (blue) and HSC70

388 antibody (green). Cells were treated with detergent extraction buffer before staining. The  
389 quantification of the percentage of cells containing HSC70 puncta in the nucleus from three  
390 independent experiments is presented (n=200). Error bars show standard deviations. **(D)** HFF  
391 cells infected with AD169 were stained at 72 hpi with DAPI (blue) and HSC70 antibody  
392 (green). **(E)** HFF cells were infected with the Merlin strain and at 5 hpi cells were treated with  
393 ROCK inhibitor (Y26732) or DMSO (as control). At 72 hpi the cells were stained with DAPI  
394 (blue) and ROCK1 antibody (red). The quantification of the percentage of cells containing  
395 ROCK1 puncta in the nucleus from three independent experiments is presented (n=400).  
396 Error bars show standard deviations. **(F)** Cells infected with Merlin strain harboring a UL32-  
397 GFP were fractionated to separate between the cytosol and the nucleus fractions. Proteins  
398 were analyzed by western blot for UL32-GFP, GAPDH (cytosolic marker) and UL57 (nuclear  
399 marker). Quantification of the ratios of nuclear and cytosolic GFP from three independent  
400 experiments is presented. Error bars show standard deviations. \* p-value<0.05, \*\* p-  
401 value<0.01 \*\*\* p-value<0.001 by two-sided student's t-test.

402

### 403 **Figure S1. ROCK1 inhibits HCMV infection**

404 **(A)** Ribosome profiling measurements of ROCK1 translation compared with protein  
405 abundance (2). **(B)** Analysis of ROCK1 RNA (upper panel) and protein (lower panel) levels.  
406 RNA was measured by real time RT-PCR and the levels were normalized to the human  
407 transcript MFGE8. ROCK1 protein was measured by western blot analysis. GAPDH was used  
408 as a loading control. **(C)** HFF cells were infected at MOI=5 with Merlin UL32-GFP strain and  
409 were either treated with ROCK inhibitor (Y27632) at 5, 24, 48 and 72 hpi, or treated with  
410 DMSO as negative control. Supernatants were collected 5 dpi and were used to infect fresh  
411 HFF cells, which were visualized by fluorescence microscopy. **(D-E)** HFF cells were infected  
412 at MOI=5 with Merlin UL32-GFP strain and at 5 hpi were either treated with ROCK  
413 inhibitors (Y26732 and H1152) or with DMSO as negative control. Supernatants were  
414 collected 5 dpi and were used to infect fresh HFF cells, GFP positive cells which were  
415 visualized by fluorescence microscopy **(D)** and quantified by FACS **(E)**. Means and error bars  
416 of triplicates are presented. \* p-value<0.05, \*\* p-value<0.01 by two-sided student's t-test. **(F)**  
417 HFF cells were transfected with an siRNA pool targeting ROCKs or a control siRNA pool

418 and infected with Merlin or AD169 HCMV strains. Proteins were extracted at the indicated  
419 times post infection and the levels of ROCK1 and IE1/2 were analyzed by western blot  
420 analysis. GAPDH was used as a loading control.

421

422 **Figure S2. The reduction in ROCK1 signal by western blot concurs with its localization**  
423 **to nuclear puncta along infection**

424 A graph showing the relative levels of ROCK1 (compared to mock) along infection as  
425 determined by western blot analysis and the percentage of nuclei in which ROCK1 was  
426 localized to nuclear puncta as quantified by microscopy (n=200).

427

428 **Figure S3. ROCK1 in HCMV infected cells is resistant to detergent treatment**

429 Mock- or Merlin- infected cells were treated with either PBS or detergent extraction buffer.  
430 Cells were then fixed, permeabilized and the localization of ROCK1 and UL57 was detected  
431 by immunofluorescence.

432

433 **Figure S4. Elevated viral titers induced by inhibition of ROCK are not due to increased**  
434 **cell viability**

435 Merlin infected HFF cells were treated with the ROCK inhibitor Y26732 or with DMSO as  
436 control, and cell viability was measured by XTT assay. A representative analysis of two  
437 independent experiments is shown. Means and error bars (showing standard deviations)  
438 represent five replicates.

439

440 **Figure S5. Treatment with the ROCK inhibitor Y26732 abolishes MLC phosphorylation**

441 HFF cells were treated with the ROCK inhibitor Y26732 for 6hrs and MLC phosphorylation  
442 was assayed by western blot using an antibody for phospho-MLC. GAPDH was used as a  
443 loading control.

444 **Materials and methods**

445

446 **Cells, viruses and treatments**

447 Human fibroblasts (CRL-1634), RPE1(CRL-4000) and the HCMV Merlin strain (VR-1590)  
448 were obtained from American Type Culture Collection (ATCC). The Merlin UL32-GFP was  
449 kindly provided by R. Stanton (41). The AD169 virus was previously described (42–44). The  
450 AD169-GFP was kindly provided by M. Messerle (45). Cells were infected at a multiplicity  
451 of infection MOI=5, unless stated otherwise, by incubation with the virus for 1hr followed by  
452 media replacement.

453 To achieve ROCK inhibition cells were treated with 10uM Y27632 (sigma) or 2uM  
454 H1152 (Santa Cruz) at the indicated times. Myosin was inhibited by treating cells with 2uM  
455 of blebbistatin. For proteasome inhibition cells were added with 10um of MG132 for 8h and  
456 proteins were extracted and analyzed by western blot.

457 To test cells viability trypsinized cells were centrifuged at 300g for 5 min and  
458 resuspended in 200ul PBS. 0.5µg/ml of *Propidium iodide* (PI) was added, incubated for 1 min  
459 and analyzed by FACS. Mock infected cells either untreated or after heat shock treatment of  
460 10min at 65°C served as negative and positive controls, respectively.

461

462 **TCID<sub>50</sub> assay**

463 10<sup>4</sup> HFF cells were plated in 96-well plates and cells were infected with 10-fold serial  
464 dilutions of supernatant from infected cells, untreated or treated with inhibitor, collected 5  
465 dpi. At 12dpi the dilutions showing cytopathic effect were evaluated by light microscopy. The  
466 TCID<sub>50</sub>/ml was calculated using the Spearman-Kaerber method (46).

467

468 **Knockdown by siRNA**

469 Cells were transfected with siRNA validated for ROCKs (ON-TARGET plus siRNA,  
470 Dharmacon) or negative control (IDT) in the presence of Lipofectamine RNAiMAX reagent

471 (Life Technologies), according to manufacturer's protocol. Infection was performed 24 hours  
472 after transfection.

473

#### 474 **Viral titer measurements using flow cytometry**

475 HFF cells were infected with Merlin UL32-GFP strain or AD169-GFP. 5dpi the supernatant  
476 was transferred to fresh HFF cells and 48hpi cells were harvested and percentage of GFP  
477 positive cells was measured by flow cytometry and normalized to the relevant control.

478

#### 479 **Western blot analysis**

480 Cells were lysed using harsh buffer (150mM Sodium Chloride, 1% Triton X100, 0.5% Sodium  
481 deoxycholate, 50mM Tris pH8.0, 0.1% SDS) or mild buffer (150mM Sodium Chloride, 0.2%  
482 Triton X100, 50mM Tris pH8.0, 0.1% SDS). Lysates were rotated at 4°C for 10 min and then  
483 centrifuged at 20,000× g for 15 min at 4°C. Samples were then separated by 4–12%  
484 polyacrylamide Bis-tris gel electrophoresis (Invitrogen), blotted onto nitrocellulose membranes  
485 and immunoblotted with primary antibodies; αROCK1 (ab134181 abcam); αGAPDH (2118S,  
486 Cell signaling); αUL44 (ICP36) (CA006 Virusys); αpp28 (CA004, Eastcoast); αHistone H2B  
487 (ab1790, Abcam); αphospho-MLC2 (C-3674, Cell Signaling Technology). Secondary  
488 antibodies were Goat anti-rabbit, Goat anti-mouse (IRDye 800CW or IRDye 680RD, Licor),  
489 or Goat anti-Rat (Alexa Fluor 680, ab175778, Abcam). Reactive bands were detected by  
490 Odyssey CLx infrared imaging system (Licor). Protein concentration was measured by  
491 Bradford assay (Sigma cat no. B6916). Protein quantification was performed using Licor  
492 software.

493

#### 494 **Cellular fractionation**

495  $2 \times 10^6$  HFF cells were seeded in a 10cm plate and either mock-infected or infected with  
496 HCMV (MOI 5). At 72 hpi, cells were fractionated using an NE-PER™ kit (thermo Fisher  
497 cat 78833). Nuclear and cytoplasmic fractions were separated on SDS gel and analyzed by  
498 Western blot.

499

500 **Immunofluorescence**

501 Cells were plated on ibidi slides and fixed in 4% paraformaldehyde for 15 min, washed in  
502 PBS (pH 7.4) and permeabilized with 0.2% Triton X-100 in PBS for 10 min, then blocked  
503 with 10% goat serum in PBS for 30 minutes. Immunostaining was performed for the detection  
504 of: ROCK1 (abcam 156284) HSC70 (Stressgen SPA-815) UL99 (Eastcoast bio CA004)  
505 UL57 (viruses corporation p1209). Cells were washed 3 times with PBS and labeled with the  
506 appropriate secondary antibody for 1 hr at room temperature; anti-rabbit Rhodamine Red-X-  
507 conjugated (Jackson ImmunoResearch 711-295-152), Cy<sup>TM</sup>2 AffiniPure Rabbit Anti-Human  
508 IgG (H+L) (Jackson ImmunoResearch 711-255-152), anti-rat Rhodamine Red-X-conjugated  
509 (Jackson ImmunoResearch 711-295-152) and FITC (sigma Anti-mouse IgG F0257). In situ  
510 detergent extraction to remove non matrix-bound proteins was performed as previously  
511 described (Christine M. Livingston et al, PLoS Pathogen 2009). Imaging was performed on a  
512 AxioObserver Z1 widefield microscope using a 40x, 63x oil objective and AxioCam 506  
513 mono camera.

514

515 **EdU staining**

516 EdU staining was performed based on (47). Briefly, HFF cells infected with Merlin for 3 days  
517 were incubated with 10uM 5-ethynyl-2'-deoxyuridine (EdU) (Jena Bioscience GmbH) for  
518 30min. Cells were then fixed with 4% formaldehyde for 10 min, Permeabilized with 0.5%  
519 Triton® X-100 for 20 min and stained with staining mix (100mM Tris pH 8.5, 1mM CuSO<sub>4</sub>,  
520 10uM fluorescent azide, 100mM ascorbic acid) for 30 min. EdU-stained cells were  
521 immunostained for ROCK1 by using standard protocol.

522

523 **Real-time PCR**

524 Total DNA was extracted using QIAamp DNA Blood Mini Kit (51104) according to the  
525 manufacturer's protocol. Real time PCR was performed using the SYBR Green PCR master-  
526 mix (ABI) on a real-time PCR system StepOnePlus (life technologies) with the following  
527 primers (forward, reverse):

528 UL55; TGGGCGAGGACAACGAA, TGAGGCTGGGAAGCTGACAT

529 B2M; TGCTGTCTCCATGTTTGATGTATCT, TCTCTGCTCCCCACCTCTAAGT

530 **XTT cell viability assay**

531 HFF cells were seeded in 96-well plates at  $5 \times 10^3$  cells/well, infected the next day with  
532 HCMV Merlin strain and treated with the ROCK inhibitor Y26732 or with DMSO as  
533 control. 4dpi cells were assayed for cell viability using the XTT-cell proliferation kit  
534 (Biological Industries, Beit Haemek, Israel) according to the manufacturer's  
535 instructions. The absorbance was measured in an ELISA plate reader at a wavelength  
536 of 470 nm and normalized to a background control.

537

538

- 540 1. Duggal NK, Emerman M. 2012. Evolutionary conflicts between viruses and restriction  
541 factors shape immunity. *Nat Rev Immunol* 12:687–695.
- 542 2. Tirosh O, Cohen Y, Shitrit A, Shani O, Le-Trilling VTK, Trilling M, Friedlander G,  
543 Tanenbaum M, Stern-Ginossar N. 2015. The Transcription and Translation Landscapes  
544 during Human Cytomegalovirus Infection Reveal Novel Host-Pathogen Interactions.  
545 *PLOS Pathog* 11:e1005288.
- 546 3. Riento K, Ridley AJ. 2003. ROCKs: multifunctional kinases in cell behaviour. *Nat Rev*  
547 *Mol Cell Biol* 4:446–456.
- 548 4. Amano M, Ito M, Kimura K, Fukata Y, Chihara K, Nakano T, Matsuura Y, Kaibuchi K.  
549 1996. Phosphorylation and activation of myosin by Rho-associated kinase (Rho-kinase). *J*  
550 *Biol Chem* 271:20246–9.
- 551 5. Schofield A V., Bernard O. 2013. Rho-associated coiled-coil kinase (ROCK) signaling  
552 and disease. *Crit Rev Biochem Mol Biol* 48:301–316.
- 553 6. Maekawa M, Ishizaki T, Boku S, Watanabe N, Fujita A, Iwamatsu A, Obinata T, Ohashi  
554 K, Mizuno K, Narumiya S. 1999. Signaling from Rho to the actin cytoskeleton through  
555 protein kinases ROCK and LIM-kinase. *Science* 285:895–8.
- 556 7. Livingston CM, Ifrim MF, Cowan AE, Weller SK. 2009. Virus-Induced Chaperone-  
557 Enriched (VICE) Domains Function as Nuclear Protein Quality Control Centers during  
558 HSV-1 Infection. *PLoS Pathog* 5:e1000619.
- 559 8. Ishizaki T, Uehata M, Tamechika I, Keel J, Nonomura K, Maekawa M, Narumiya S.  
560 2000. Pharmacological properties of Y-27632, a specific inhibitor of rho-associated  
561 kinases. *Mol Pharmacol* 57:976–83.
- 562 9. Sharon-Friling R, Shenk T. 2014. Human cytomegalovirus pUL37x1-induced calcium  
563 flux activates PKC , inducing altered cell shape and accumulation of cytoplasmic vesicles.  
564 *Proc Natl Acad Sci* 111:E1140–E1148.
- 565 10. Stanton RJ, Baluchova K, Dargan DJ, Cunningham C, Sheehy O, Seirafian S, McSharry  
566 BP, Neale ML, Davies JA, Tomasec P, Davison AJ, Wilkinson GWG. 2010.



- 567 Reconstruction of the complete human cytomegalovirus genome in a BAC reveals RL13  
568 to be a potent inhibitor of replication. *J Clin Invest* 120:3191–3208.
- 569 11. Sasaki Y, Suzuki M, Hidaka H. The novel and specific Rho-kinase inhibitor (S)-(+)-2-  
570 methyl-1-[(4-methyl-5-isoquinoline)sulfonyl]-homopiperazine as a probing molecule for  
571 Rho-kinase-involved pathway. *Pharmacol Ther* 93:225–32.
- 572 12. Ryckman BJ, Rainish BL, Chase MC, Borton JA, Nelson JA, Jarvis MA, Johnson DC.  
573 2008. Characterization of the Human Cytomegalovirus gH/gL/UL128-131 Complex That  
574 Mediates Entry into Epithelial and Endothelial Cells. *J Virol* 82:60–70.
- 575 13. Murrell I, Tomasec P, Wilkie GS, Dargan DJ, Davison AJ, Stanton RJ. 2013. Impact of  
576 Sequence Variation in the UL128 Locus on Production of Human Cytomegalovirus in  
577 Fibroblast and Epithelial Cells. *J Virol* 87:10489–10500.
- 578 14. Kopito RR. 2000. Aggresomes, inclusion bodies and protein aggregation. *Trends Cell Biol*  
579 10:524–30.
- 580 15. Burch AD, Weller SK. 2004. Nuclear sequestration of cellular chaperone and proteasomal  
581 machinery during herpes simplex virus type 1 infection. *J Virol* 78:7175–85.
- 582 16. Burch AD, Weller SK. 2005. Herpes simplex virus type 1 DNA polymerase requires the  
583 mammalian chaperone hsp90 for proper localization to the nucleus. *J Virol* 79:10740–9.
- 584 17. Livingston CM, DeLuca NA, Wilkinson DE, Weller SK. 2008. Oligomerization of ICP4  
585 and rearrangement of heat shock proteins may be important for herpes simplex virus type  
586 1 prereplicative site formation. *J Virol* 82:6324–36.
- 587 18. Li L, Johnson LA, Dai-Ju JQ, Sandri-Goldin RM. 2008. Hsc70 Focus Formation at the  
588 Periphery of HSV-1 Transcription Sites Requires ICP27. *PLoS One* 3:e1491.
- 589 19. Tran K, Mahr JA, Spector DH. 2010. Proteasome Subunits Relocalize during Human  
590 Cytomegalovirus Infection, and Proteasome Activity Is Necessary for Efficient Viral Gene  
591 Transcription. *J Virol* 84:3079–3093.
- 592 20. Lin S-R, Jiang MJ, Wang H-H, Hu C-H, Hsu M-S, Hsi E, Duh C-Y, Wang S-K. 2013.  
593 Human cytomegalovirus UL76 elicits novel aggresome formation via interaction with S5a  
594 of the ubiquitin proteasome system. *J Virol* 87:11562–78.

- 595 21. Watanabe K, Ueno M, Kamiya D, Nishiyama A, Matsumura M, Wataya T, Takahashi JB,  
596 Nishikawa S, Nishikawa S, Muguruma K, Sasai Y. 2007. A ROCK inhibitor permits  
597 survival of dissociated human embryonic stem cells. *Nat Biotechnol* 25:681–686.
- 598 22. Charras G, Paluch E. 2008. Blebs lead the way: how to migrate without lamellipodia. *Nat*  
599 *Rev Mol Cell Biol* 9:730–736.
- 600 23. Wilkie AR, Lawler JL, Coen DM. 2016. A Role for Nuclear F-Actin Induction in Human  
601 Cytomegalovirus Nuclear Egress. *MBio* 7:e01254-16.
- 602 24. Varnum SM, Streblow DN, Monroe ME, Smith P, Auberry KJ, Pasa-Tolic L, Wang D,  
603 Camp DG, Rodland K, Wiley S, Britt W, Shenk T, Smith RD, Nelson JA, Nelson JA.  
604 2004. Identification of proteins in human cytomegalovirus (HCMV) particles: the HCMV  
605 proteome. *J Virol* 78:10960–6.
- 606 25. Zheng K, Xiang Y, Wang X, Wang Q, Zhong M, Wang S, Wang X, Fan J, Kitazato K,  
607 Wang Y. 2014. Epidermal growth factor receptor-PI3K signaling controls cofilin activity  
608 to facilitate herpes simplex virus 1 entry into neuronal cells. *MBio* 5:e00958-13.
- 609 26. Frampton AR, Stolz DB, Uchida H, Goins WF, Cohen JB, Glorioso JC. 2007. Equine  
610 herpesvirus 1 enters cells by two different pathways, and infection requires the activation  
611 of the cellular kinase ROCK1. *J Virol* 81:10879–89.
- 612 27. Valderrama F, Cordeiro J V, Schleich S, Frischknecht F, Way M. 2006. Vaccinia virus-  
613 induced cell motility requires F11L-mediated inhibition of RhoA signaling. *Science*  
614 311:377–81.
- 615 28. Melnychuk RM, Streblow DN, Smith PP, Hirsch AJ, Pancheva D, Nelson JA. 2004.  
616 Human cytomegalovirus-encoded G protein-coupled receptor US28 mediates smooth  
617 muscle cell migration through Galpha12. *J Virol* 78:8382–91.
- 618 29. McCormick D, Lin Y-T, Grey F. 2018. Identification of Host Factors Involved in Human  
619 Cytomegalovirus Replication, Assembly, and Egress Using a Two-Step Small Interfering  
620 RNA Screen. *MBio* 9:e00716-18.
- 621 30. Murrell M, Oakes PW, Lenz M, Gardel ML. 2015. Forcing cells into shape: the mechanics  
622 of actomyosin contractility. *Nat Rev Mol Cell Biol* 16:486–498.

- 623 31. Sampaio KL, Cavnac Y, Stierhof Y-D, Sinzger C. 2005. Human cytomegalovirus  
624 labeled with green fluorescent protein for live analysis of intracellular particle movements.  
625 *J Virol* 79:2754–67.
- 626 32. Bosse JB, Enquist LW. 2016. The diffusive way out: Herpesviruses remodel the host  
627 nucleus, enabling capsids to access the inner nuclear membrane. *Nucleus* 7:13–19.
- 628 33. Forest T, Barnard S, Baines JD. 2005. Active intranuclear movement of herpesvirus  
629 capsids. *Nat Cell Biol* 7:429–431.
- 630 34. Feierbach B, Piccinotti S, Bisher M, Denk W, Enquist LW. 2006. Alpha-Herpesvirus  
631 Infection Induces the Formation of Nuclear Actin Filaments. *PLoS Pathog* 2:e85.
- 632 35. Bosse JB, Hogue IB, Feric M, Thiberge SY, Sodeik B, Brangwynne CP, Enquist LW.  
633 2015. Remodeling nuclear architecture allows efficient transport of herpesvirus capsids by  
634 diffusion. *Proc Natl Acad Sci U S A* 112:E5725-33.
- 635 36. Wilkie AR, Sharma M, Pesola JM, Ericsson M, Fernandez R, Coen DM. 2018. A Role for  
636 Myosin Va in Human Cytomegalovirus Nuclear Egress. *J Virol* 92:e01849-17.
- 637 37. Simon DN, Wilson KL. 2011. The nucleoskeleton as a genome-associated dynamic  
638 “network of networks.” *Nat Rev Mol Cell Biol* 12:695–708.
- 639 38. de Lanerolle P, Johnson T, Hofmann WA. 2005. Actin and myosin I in the nucleus: what  
640 next? *Nat Struct Mol Biol* 12:742–746.
- 641 39. Visa N, Percipalle P. 2010. Nuclear functions of actin. *Cold Spring Harb Perspect Biol*  
642 2:a000620.
- 643 40. Li G, Kamil JP. 2016. Viral Regulation of Cell Tropism in Human Cytomegalovirus. *J*  
644 *Virol* 90:626–9.
- 645 41. Stanton RJ, Baluchova K, Dargan DJ, Cunningham C, Sheehy O, Seirafian S, McSharry  
646 BP, Neale ML, Davies JA, Tomasec P, Davison AJ, Wilkinson GWG. 2010.  
647 Reconstruction of the complete human cytomegalovirus genome in a BAC reveals RL13  
648 to be a potent inhibitor of replication. *J Clin Invest* 120:3191–3208.
- 649 42. Le VTK, Trilling M, Hengel H. 2011. The Cytomegaloviral Protein pUL138 Acts as  
650 Potentiator of Tumor Necrosis Factor (TNF) Receptor 1 Surface Density To Enhance

- 651 ULb'-Encoded Modulation of TNF- Signaling. *J Virol* 85:13260–13270.
- 652 43. Seidel E, Le VTK, Bar-On Y, Tsukerman P, Enk J, Yamin R, Stein N, Schmiedel D,  
653 Oiknine Djian E, Weisblum Y, Tirosh B, Stastny P, Wolf DG, Hengel H, Mandelboim O.  
654 2015. Dynamic Co-evolution of Host and Pathogen: HCMV Downregulates the Prevalent  
655 Allele MICA\*008 to Escape Elimination by NK Cells. *Cell Rep*.
- 656 44. Rölle A, Pollmann J, Ewen E-M, Le VTK, Halenius A, Hengel H, Cerwenka A. 2014. IL-  
657 12-producing monocytes and HLA-E control HCMV-driven NKG2C+ NK cell  
658 expansion. *J Clin Invest* 124:5305–5316.
- 659 45. Borst E-M, Messerle M. 2005. Analysis of Human Cytomegalovirus oriLyt Sequence  
660 Requirements in the Context of the Viral Genome. *J Virol* 79:3615–3626.
- 661 46. Darling AJ, Boose JA, Spaltro J. 1998. Virus assay methods: accuracy and validation.  
662 *Biologicals* 26:105–10.
- 663 47. Jao CY, Salic A. 2008. Exploring RNA transcription and turnover in vivo by using click  
664 chemistry. *Proc Natl Acad Sci* 105:15779–15784.
- 665
- 666